Published in final edited form as:
*Nano Lett*. 2009 April ; 9(4): 1555–1558. doi:10.1021/nl803647n.

# Tailoring the Structure of Nanopyramids for Optimal Heat Generation

**Warefta Hasan**[†], **Christopher L. Stender**[†], **Min Hyung Lee**[†], **Colleen L. Nehl**[†], **Jeunghoon Lee**[†,+], and **Teri W. Odom**[†,‡,*]

† *Department of Chemistry, Northwestern University, 2145 Sheridan Road, Evanston, Illinois 60208-3113*

‡ *Department of Materials Science and Engineering, Northwestern University, 2145 Sheridan Road, Evanston, Illinois 60208-3113*

This paper investigates how structural features of noble metal nanoparticles affect their photothermal properties. Using PEEL, we fabricated a range of Au nanopyramid-like particles with surface plasmon resonances tunable from visible to near-infrared wavelengths. By systematically varying geometric parameters including size, shell thickness, and presence or absence of tips, we determined which factors were most important in heat generation. For solutions with the same Au content, we discovered that pyramidal particles with thin shells and having sharp tips showed the largest photothermal response.

Designing nanoparticles (NPs) with high efficiencies for photothermal cancer therapy requires a thorough understanding of how their structural parameters affect heat generation. When illuminated with light, noble metal NPs can generate and dissipate heat to the surrounding environment, an effect that is called a photothermal response.[1] Heating is most efficient when the energy of the incident light is close to a surface plasmon (SP) resonance of the metal NP.[2,3] Depending on the size and shape of the NP, light can either be scattered (the dominate process for NPs > 100 nm) or absorbed (the dominate process for NPs < 100 nm).[4,5] In particular, heat dissipated by spherical Au NPs after absorption of visible light has been used for thermal imaging of proteins attached to cells,[6] releasing drugs from a capsule containing Au NPs,[7] and ablating cancer cells.[8,9]

For the photothermal response of NPs to be effective for *in vivo* therapeutic applications, light must penetrate 6–9 mm into tissue without damaging cellular components and without being absorbed by hemoglobin or other chromophores.[10] This property can be achieved using NPs that absorb in the biologically relevant near-infrared (NIR, 650 – 900 nm) window. Au NPs are ideal candidates for photothermal therapy because: (1) their optical properties can be easily tuned in the NIR; (2) their *in vivo* toxicity is low;[11–13] and (3) their surfaces can be easily modified with antibodies to target specific receptors.[14] Au nanorods, nanocages, core-shell particles, and $Ag/Fe_3O_4/SiO_2$ nanoshells support dipolar resonances in the NIR that can be excited to generate heat upon laser irradiation.[15–18] The mechanism of heat generation by Au nanorods has been identified by dynamical photothermal studies using ultrafast transient absorption spectroscopy.[19] Additionally, Au-based NPs have been shown to target and ablate cancer cells under irradiation for 5–7 min at wavelengths between 800 – 820 nm.[14] The mechanism for cell death by a photothermal response has been studied using Au nanorods; cell

*To whom correspondence should be addressed. E-mail: todom@northwestern.edu.
+Present address: Department of Chemistry and Biochemistry, Boise State University, 1910 University Drive, Boise, ID 83725-1520

SUPPORTING INFORMATION: Effect of laser power and shell thickness (for tipless pyramids) on the photothermal response of nanopyramid suspensions. This material is available free of charge via the Internet at http://pubs.acs.org.

damage was observed to be ten times greater when the rods were attached to the surface compared to being internalized.[20] Also, the minimum number of Au NPs (nanocages with edge lengths of 65 nm or colloids with diameters of 40 nm) per cell required for cell death was found to be 450 ± 140.[21] There has, however, only been limited experimental work correlating the size, shape, and local environment of NPs with their photothermal response.

Here we have used fabricated pyramidal particles[22–25] as a platform to evaluate quantitatively which structural parameters are most important for heat generation. Nanopyramids are an ideal system for this study because their geometric features—size, shell thickness, and tip structure—can be easily tailored. For these investigations, we fabricated pyramids with two different base diameters ($d$ = 175 nm and 350 nm), two shell thicknesses ($t$ = 20 nm and $t$ = 60 nm), and two shapes (with tips (WT) and without tips (TL)). Specifically, we compared the photothermal response of four different pyramidal structures in aqueous solution: (1) thin ($t$ = 20 nm) with tips (WT 20); (2) thick ($t$ = 60 nm) with tips (WT 60); (3) thin without tips (TL 20); and (4) thick without tips (TL 60) (Fig. 1).

To correlate the different nanopyramid structures and their photothermal response, we measured the bulk temperature increase of the particles dispersed in water. We expect the local temperature on the surface of the pyramids, however, to be much higher than the temperature increase of the solution. For all photothermal measurements, 100-μL aliquots from a stock suspension were analyzed simultaneously by UV-Vis spectroscopy and inductively coupled plasma-atomic emission spectroscopy (ICP-AES). Thus, the solutions were comparable in optical density and the total amount of gold present. To ensure that the heating effects we observed were primarily from structural changes, NP suspensions having the *same Au content* in parts per million (1 ppm = 1 mg/L) were compared. A fs-pulsed Ti:Sapphire laser (550 mW and 17 W/cm$^2$) tuned to 760 nm was used as the excitation source. This wavelength was selected based on the intensity at which the extinction spectra of the nanopyramid samples were similar. A thermocouple immersed in the quartz cuvette was used to monitor the temperature increase upon laser exposure; the starting temperature of the suspension was 27 °C. Samples were irradiated for 6 min to allow enough time for the temperature to plateau and to facilitate a comparison with previous reports.[15–18] The photothermal response of each nanopyramid suspension was measured on three consecutive days; the standard deviation of these measurements was used to determine the error bars for each temperature measurement.

To determine the effect of the nanopyramid *size* on the photothermal response, we tested Au pyramids with $d$ = 175 nm and $d$ = 350 nm and both having thicknesses $t$ = 20 nm. Figure 2A indicates that the UV-Vis extinction spectra of the nanopyramid suspensions at the irradiation wavelength were similar. The concentration of 175-nm pyramids was $2.42 \times 10^7$ particles/mL, and 350-nm pyramids was $6.06 \times 10^6$ particles/mL, both equivalent to 0.15 ppm of Au. The temperature rise for the larger pyramids was 3 °C higher than that for the smaller pyramids (Fig. 2B). This observation is significant because previous reports have shown that 80-nm Au colloids have a higher absorption efficiency than 400-nm Au colloids.[26] To understand our results, we considered the broad features in the extinction, where 175-nm pyramids have a single resonance centered at 820 nm, while 350-nm pyramids displayed a broad resonance starting around 650 nm. Based on previous experimental and theoretical studies, the 820-nm resonance of 175-nm pyramids is dipolar in nature, whereas the 650-nm resonance of 350-nm pyramids is quadrupolar in character.[27,28] Using 760-nm light, we excited the dipole for small pyramids and the quadrupole for large pyramids. Our results suggest that quadrupolar resonances can be as efficient as dipolar resonances at producing heat. Also, we examined the effect of laser power on the photothermal response of the pyramids by testing three laser powers (250 mW, 550 mW, and 800 mW). For these studies, we used WT 20 pyramids with a Au content 0.15 ppm and irradiated them for 6 min. We found that heat generation was proportional

to laser power (Fig. S1) and, in addition, did not observe significant differences in the photothermal response of nanopyramids between continuous wave and pulsed laser excitation.

To correlate the effects of *shell thickness* and *tip structure* on heating, only pyramids with $d$ = 350 nm were considered. We have shown that thinner pyramids ($t$ = 60 nm) have plasmon resonances that are red-shifted compared to thicker pyramids ($t$ = 110 nm) with 350-nm diameters.[28] Figure 3A shows that this trend was also observed for pyramids with $t$ = 20 nm and $t$ = 60 nm. To determine the effect of shell thickness on the temperature increase, WT 20 and WT 60 pyramids with similar optical densities and Au content of 0.6 ppm were tested. Suspensions of WT 20 particles ($2.53 \times 10^8$ particles/mL) heated up approximately 4 °C more than suspensions of WT 60 ($8.44 \times 10^7$ particles/mL) upon irradiation (Fig. 3B). A similar trend was also observed for tipless nanopyramids with different thicknesses (Fig. S2).

Figure 4 compares the effect of a *tip* on the photothermal response of nanopyramid suspensions. Truncations of the tip of a pyramid have been predicted to red-shift the dipolar and quadrupolar plasmon resonances.[28] Our observations are in agreement that the quadrupole excitation of the TL pyramids was red-shifted compared to the WT pyramids (Fig. 4A). Controlling for the same amount of Au (0.6 ppm), WT 20 particles heated up the bulk solution 4 °C more than the TL 20 pyramids (Fig. 4B). These results suggest that the presence of sharp features, such as the nanopyramid tip, is important in heat production by nanoparticles.

Figure 5 summarizes the photothermal response of nanopyramid suspensions with four different structures and different amounts of Au content. At an Au content of 0.6 ppm (Fig. 5, dotted line), thin pyramids with tips (WT 20) heated the 100-μL water volume approximately 5 °C more than the other pyramidal structures. The temperature increase per ppm of Au (slope of the line) for WT 20 was 6.67 °C/ppm while for thin pyramids without tips (TL 20), it was 6.16 °C/ppm. In contrast, thick pyramids with tips (WT 60) generated a temperature increase of 2.97 °C/ppm and the ones without tips (TL 60) 2.64 °C/ppm. These measurements indicate that (1) the presence of a tip and (2) the thickness of the Au shells are important structural parameters for designing nanoparticles for photothermal therapy. Also, the temperature increase per ppm of Au of thin pyramids is higher than that of thicker pyramids, which may be explained by considering the surface-area-to-volume ratio of the two structures. Fourier's law of heat conduction states that the rate of heat transfer is proportional to the surface area normal to the temperature gradient.[29] If the thermal gradient occurs at the nanopyramid-solution interface, a higher surface-area-to-volume ratio should increase heat transfer rate, which is what we observed for thin shells compared to thick ones.

Finally, after screening the photothermal response for different pyramidal structures, we investigated the WT 20 pyramids, which generated the most heat, under near-physiological conditions: 37 °C and pH 7.4 (phosphate buffer). Under these conditions, a temperature increase of 8 °C for 0.45 ppm Au ($1.82 \times 10^7$ particles/mL) over 6 min was measured (Fig. 6). Although the absolute value of the increase is less than that observed in water (Fig. 4), this response can be attributed to the difference in heat capacities of water (75.33 $Jmol^{-1}K^{-1}$) and phosphate buffer (187 $Jmol^{-1}K^{-1}$),[30] and is still sufficient enough to induce cell death.[13,31] The time required for the nanopyramid suspension to return to the starting temperature once the laser irradiation was turned off was 30 min.

In conclusion, we have compared the photothermal response of a wide range of different pyramidal nanoparticles with various shapes, sizes, and shell thicknesses. We are the first to quantify how heat generation by nanoparticles in bulk aqueous media depends on the shape and optical properties of the nanoparticles. This work is important because it highlights critical design aspects (sharp features and thin shells) that can be used to optimize heat generation of

Au nanoparticles. Photothermal therapy can possibly be made more efficient through use of highly tailorable particles, such as nanopyramids.

## Supplementary Material

Refer to Web version on PubMed Central for supplementary material.

## Acknowledgements

This work was supported in part by the Center of Cancer Nanotechnology Excellence initiative of the NIH National Cancer Institute under Award Number U54CA119341, the NSF MRSEC program at Northwestern University (DMR-0520513), the David and Lucile Packard Foundation, and the NIH Director's Pioneer Award (DP1OD003899). This work used the NU*ANCE* Center facilities, which are supported by NSF-MRSEC, NSF-NSEC and the Keck Foundation.

## References

1. Link S, El-Sayed MA. J Phys Chem B 1999;103:4212–4217.
2. Chou CH, Chen CD, Wang CRC. J Phys Chem B 2005;109:11135–11138. [PubMed: 16852358]
3. Eustis S, El-Sayed MA. Chem Soc Rev 2006;35:209–217. [PubMed: 16505915]
4. Jain PK, Lee KS, El-Sayed IH, El-Sayed MA. J Phys Chem B 2006;110:7238–7248. [PubMed: 16599493]
5. Hu M, Chen J, Li ZY, Au L, Hartland GV, Li X, Marquez M, Xia Y. Chem Soc Rev 2006;35:1084–1094. [PubMed: 17057837]
6. Cognet L, Tardin C, Boyer D, Choquet D, Tamarat P, Lounis B. Proc Natl Acad Sci 2003;100:11350–11355. [PubMed: 13679586]
7. Bikram M, Gobin AM, Whitmire RE, West JL. J of Contr Rel 2007;123:219–227.
8. Pitsillides CM, Joe EK, Wei XB, Anderson RR, Lin CP. Biophys J 2003;84:4023–4032. [PubMed: 12770906]
9. Pissuwan D, Valenzuela SM, Cortie MB. Trends Biotechnol 2006;24:62–67. [PubMed: 16380179]
10. Weissleder R. Nat Biotechnol 2001;19:316–317. [PubMed: 11283581]
11. Connor EE, Mwamuka J, Gole A, Murphy CJ, Wyatt MD. Small 2005;1:325–327. [PubMed: 17193451]
12. Pan Y, Neuss S, Leifert A, Fischler M, Wen F, Simon U, Schmid G, Brandau W, Jahnen-Dechent W. Small 2007;3:1941–1949. [PubMed: 17963284]
13. Huff TB, Tong L, Zhao Y, Hansen MN, Cheng JX, Wei A. Nanomedicine 2007;2:125–132. [PubMed: 17716198]
14. Huang X, Jain PK, El-Sayed IA, El-Sayed MA. Nanomedicine 2007;2:681–693. [PubMed: 17976030]
15. Huang X, El-Sayed IH, Qian W, El-Sayed MA. J Am Chem Soc 2006;128:2115–2120. [PubMed: 16464114]
16. Hirsch LR, Stafford RJ, Bankson JA, Sershen SR, Rivera B, Price RE, Hazle JD, Halas NJ, West JL. Proc Natl Acad Sci 2003;100:13549–13554. [PubMed: 14597719]
17. Chen J, Wang D, Xi J, Au L, Siekkinen A, Warsen A, Li ZY, Zhang H, Xia Y, Li X. Nano Lett 2007;7:1318–1322. [PubMed: 17430005]
18. Chen M, Kim YN, Lee HM, Li C, Cho SO. J Phys Chem C 2008;112:8870–8874.
19. Links S, El-Sayed MA. J Phys Chem B 1999;103:8410–8426.
20. Tong L, Zhao Y, Huff TB, Hansen MN, Wei A, Cheng JX. Adv Mater 2007;19:3136–3141.
21. Au L, Zheng D, Zhou F, Li ZY, Li X, Xia Y. ACS Nano 2008;2:1645–1652. [PubMed: 19206368]
22. Henzie J, Kwak E, Odom TW. Nano Lett 2005;5:1199–1202. [PubMed: 16178210]
23. Lee J, Hasan W, Stender CL, Odom TW. Acc Chem Res 2008;41:1762–1771. [PubMed: 18803410]
24. Stender CL, Nehl CL, Hasan W, Odom TW. In preparation.
25. Henzie J, Barton JE, Stender CL, Odom TW. Acc Chem Res 2006;39:249–257. [PubMed: 16618092]
26. Harris N, Ford MJ, Cortie MB. J Phys Chem B 2006;110:10701–10707. [PubMed: 16771316]

27. Henzie J, Shuford KL, Kwak E, Schatz GC, Odom TW. J Phys Chem B 2006;110:14028–14031. [PubMed: 16854094]
28. Shuford KL, Lee J, Odom TW, Schatz GC. J Phys Chem C 2008;112:6662–6666.
29. Middleman, S. A introduction to mass and heat transfer. Wiley; 1998.
30. In *CRC Index*.
31. Huang X, Jain PK, El-Sayed I, El-Sayed MA. Lasers in Med Sci 2007;23:217–228. [PubMed: 17674122]

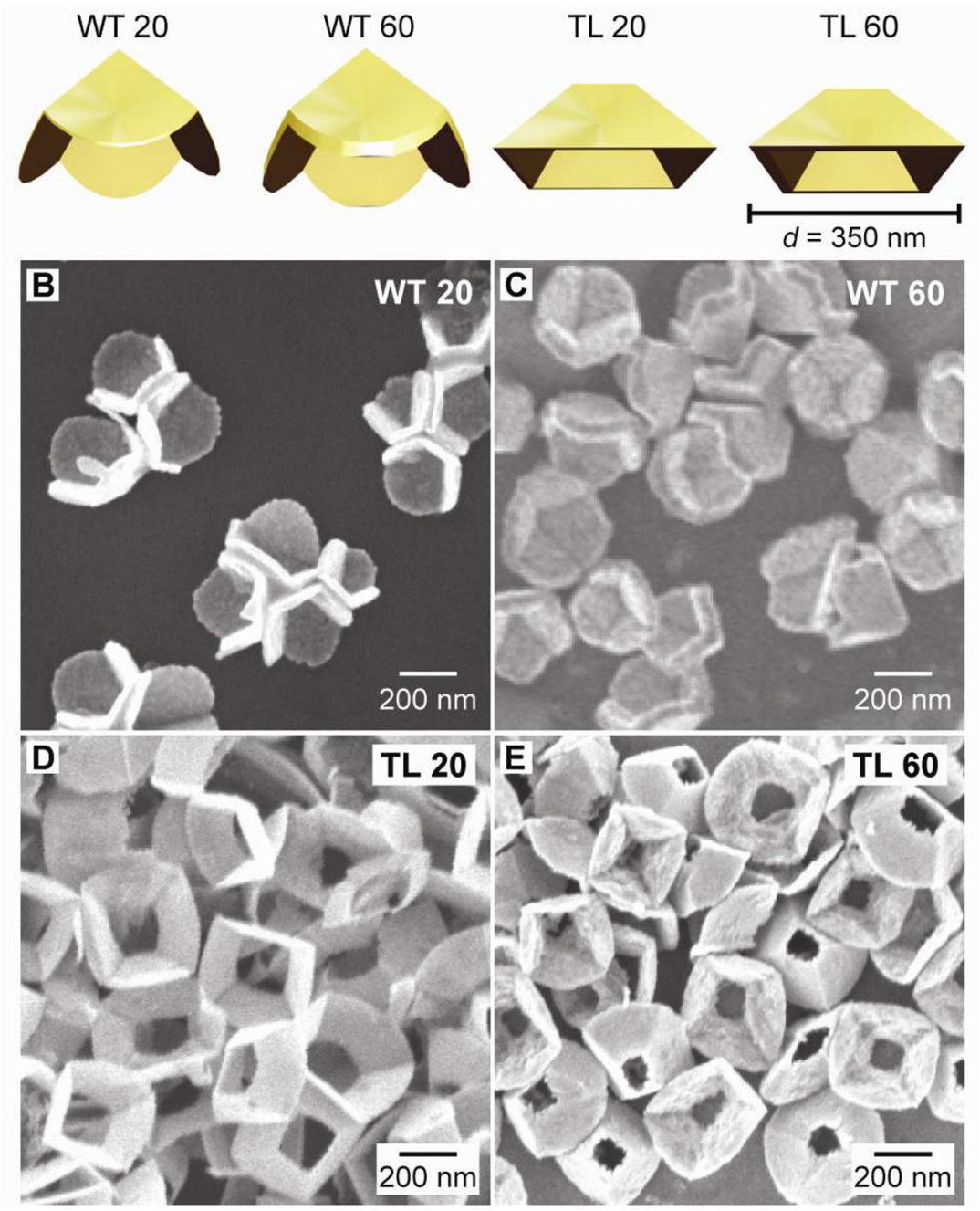


**Figure 1. Pyramidal structures investigated for their photothermal response**

**(A)** Cartoon images of the different types of Au nanopyramids (to scale). SEM images of nanopyramids that are **(B)** thin with tips (WT 20), **(C)** thick with tips (WT 60), **(D)** thin without tips (TL 20), and **(E)** thick without tips (TL 60).

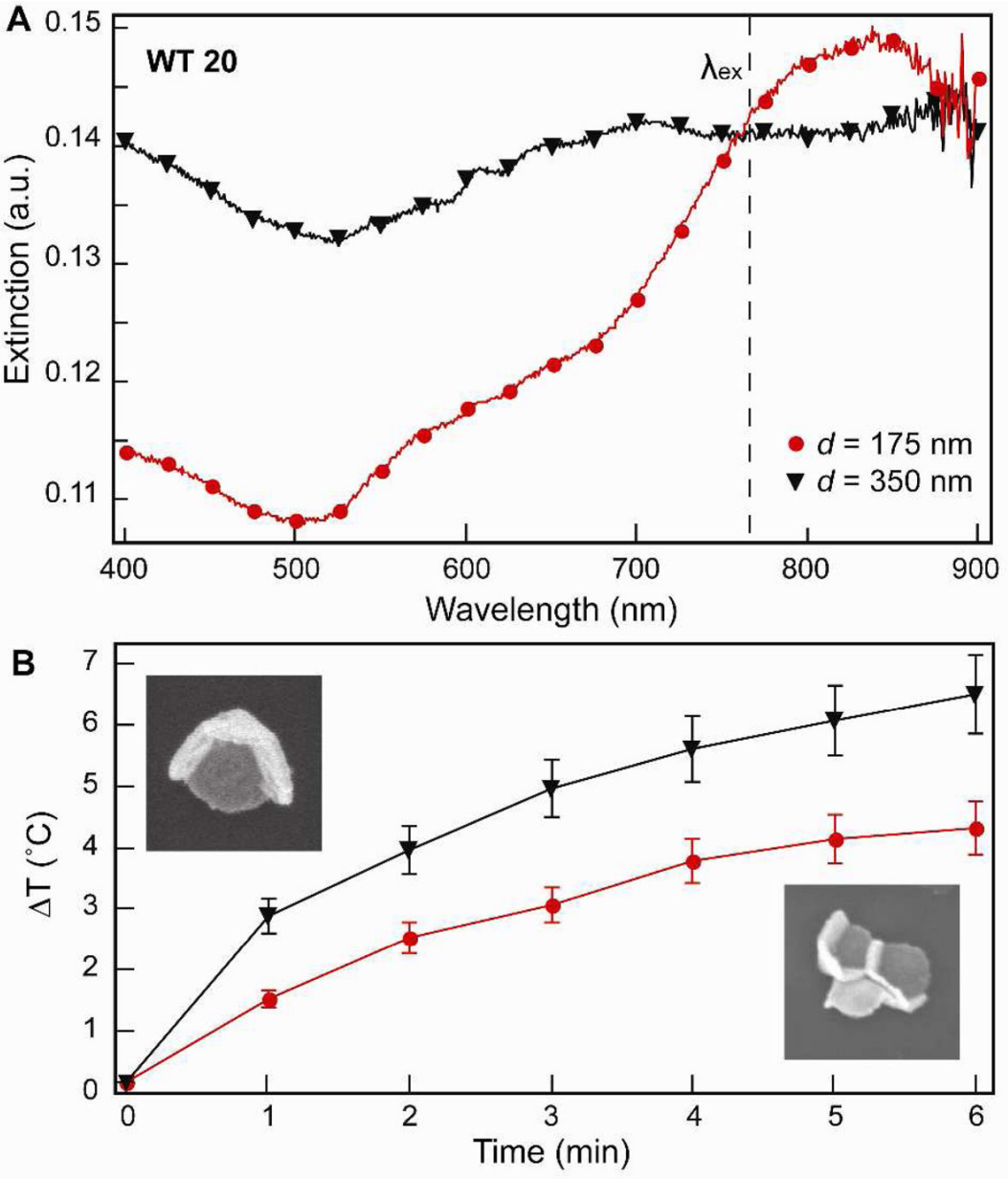


**Figure 2. Effect of nanopyramid size on the photothermal response**

**(A)** Extinction spectra of nanopyramids with different sizes (*d* = 175 and 350 nm). **(B)** Photothermal response of nanopyramids with different sizes with the same amount of Au (0.15 ppm). SEM images are 400 nm × 400 nm.

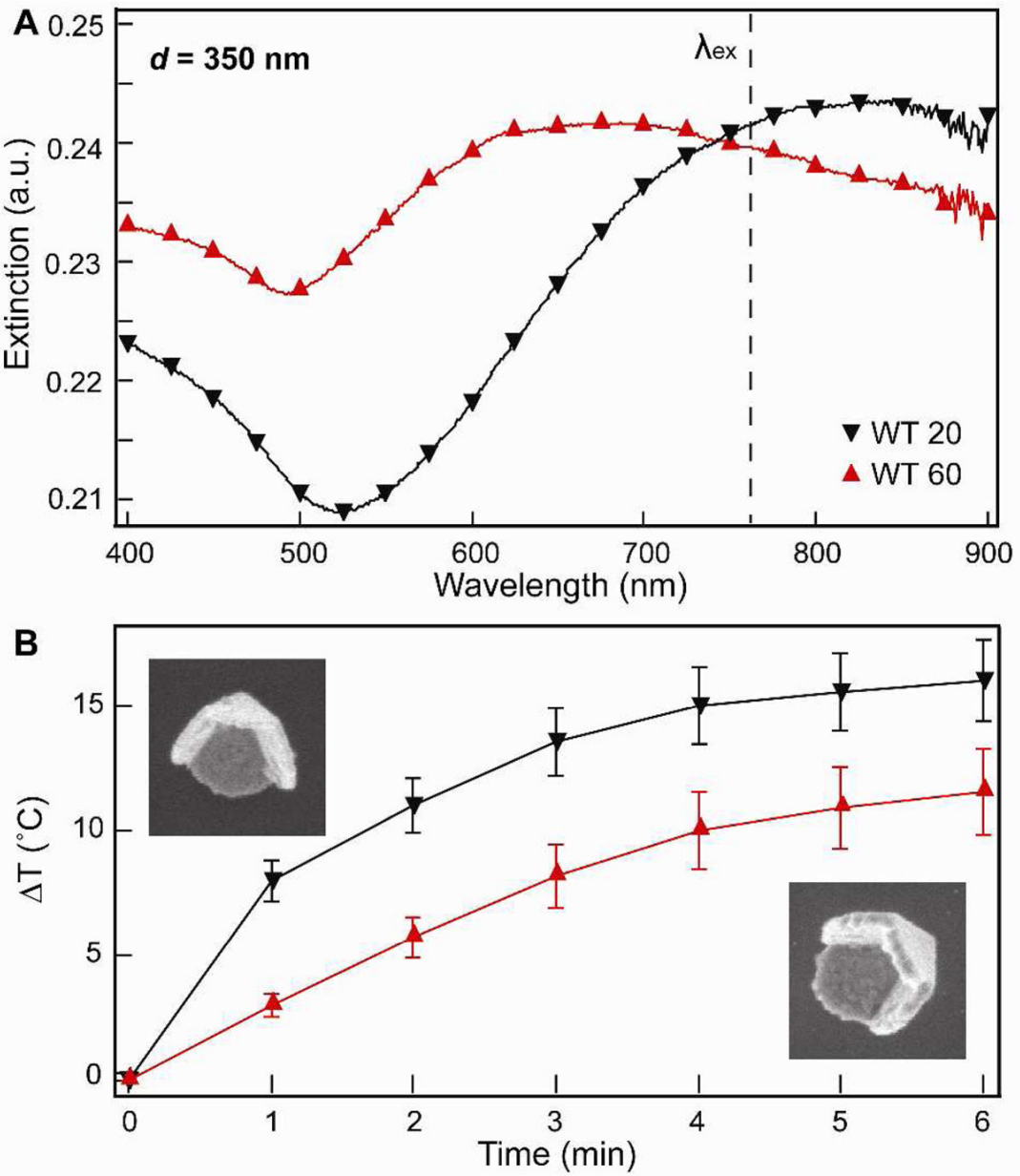


**Figure 3. Effect of shell thickness on the photothermal response**

**(A)** Extinction spectra of Au nanopyramids (*d* = 350 nm) with different shell thicknesses. **(B)** Photothermal response of WT 20 and WT 60 nanopyramids containing the same amount of Au (0.6 ppm). SEM images are 400 nm × 400 nm.

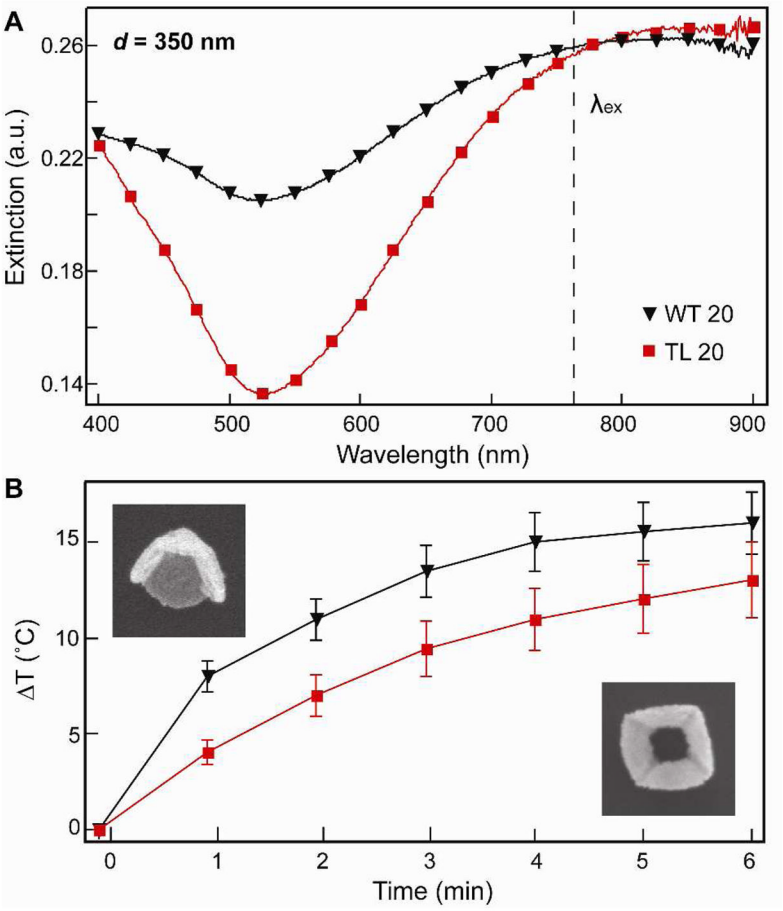


**Figure 4. Effect of a tip on the photothermal response**

**(A)**Extinction spectra of Au nanopyramids (*d* = 350 nm) with and without tips. **(B)** Photothermal response of WT 20 and TL 20 nanopyramids containing the same amount of Au (0.6 ppm). SEM images are 400 nm × 400 nm.

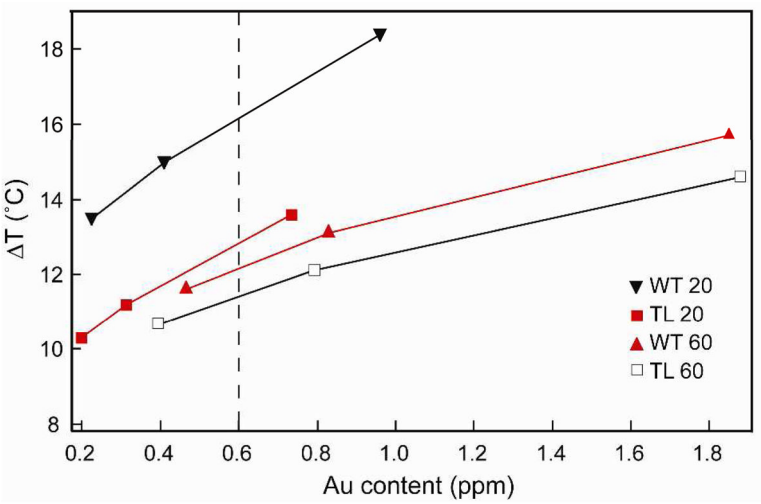


**Figure 5.**
Plot correlating the photothermal response of nanopyramids with different amounts of Au for each of the four pyramidal structures.

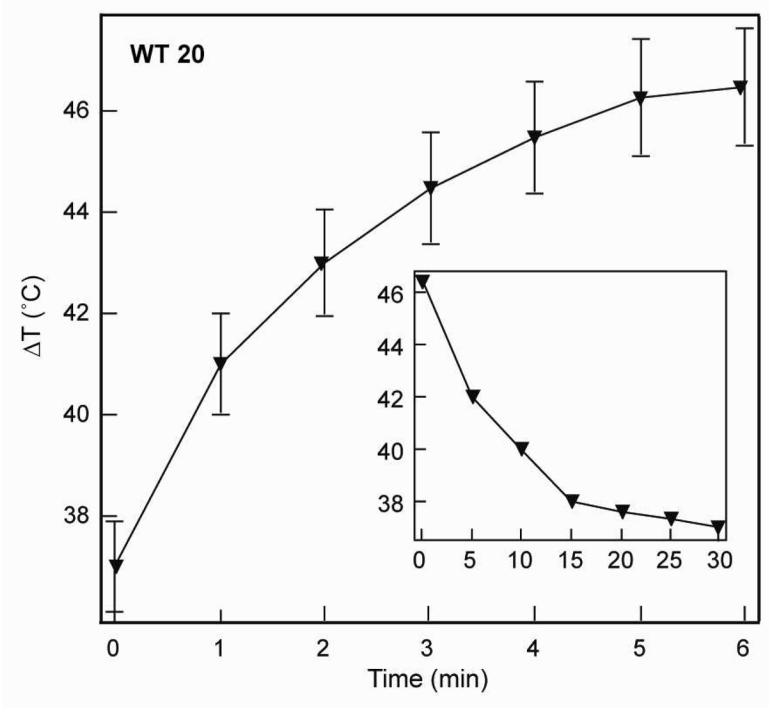


**Figure 6.**
Photothermal response of thin nanopyramids with tips in near-physiological conditions.